# Growth of graphene underlayers by chemical vapor deposition

Mopeli Fabiane,[1] Saleh Khamlich,[1] Abdulhakeem Bello,[1] Julien Dangbegnon,[1] Damilola Momodu,[1] A. T. Charlie Johnson,[2] and Ncholu Manyala[1,a]

[1]*Department of Physics, Institute of Applied Materials, SARChI Chair in Carbon Technology and Materials, University of Pretoria, Pretoria 0028, South Africa*

[2]*Department of Physics and Astronomy, University of Pennsylvania, Philadelphia, Pennsylvania 19104, USA*

(Received 2 August 2013; accepted 12 November 2013; published online 21 November 2013)

We present a simple and very convincing approach to visualizing that subsequent layers of graphene grow between the existing monolayer graphene and the copper catalyst in chemical vapor deposition (CVD). Graphene samples were grown by CVD and then transferred onto glass substrates by the *bubbling method* in two ways, either direct-transfer (DT) to yield poly (methyl methacrylate) (PMMA)/graphene/glass or (2) inverted transfer (IT) to yield graphene/PMMA/glass. Field emission scanning electron microscopy (FE-SEM) and atomic force microscopy (AFM) were used to reveal surface features for both the DT and IT samples. The results from FE-SEM and AFM topographic analyses of the surfaces revealed the underlayer growth of subsequent layers. The subsequent layers in the IT samples are visualized as 3D structures, where the smaller graphene layers lie above the larger layers stacked in a concentric manner. The results support the formation of the so-called "inverted wedding cake" stacking in multilayer graphene growth.  [http://dx.doi.org/10.1063/1.4834975]

## I. INTRODUCTION

Progress with the synthesis of large-area graphene, a two-dimensional (2D) material with exotic physical properties, has fostered new applications for it, such as transparent electrodes and high-frequency transistors.[1–3] Currently, large-area graphene is synthesized on different metal catalytic substrates[4–8] and many results have been summarized in the review by Mattevi *et al.* of graphene deposited on Cu by chemical vapor deposition (CVD).[9] The concept of dissolving carbon in other materials and then dissociating it to form graphene layers was first proposed by Acheson when he discovered *Carborundum* or silicon carbide.[10,11] This led to further research on the formation of graphite layers on metals. For example, graphite layers were first observed on Ni surfaces when these surfaces were exposed to carbon sources.[12,13] More elaborate was the work of Shelton *et al*. in 1974.[14] They studied the segregation of carbon on the (111) surface of Ni containing ∼0.3 at% carbon solution using Auger spectroscopy and low-energy electron diffraction (LEED). At high, intermediate and low temperatures, three distinct equilibrium states during segregation were identified, which were explained as segregated carbon phases. In this way, the gas phase at high temperature, the carbon monolayer (graphene) phase at intermediate temperature having a graphite basal plane, and several layers of graphite at low temperatures were determined, providing a systematic and controllable way to grow graphite monolayer and multilayers from the out-diffusion of the carbon impurities in the bulk solid solution. Most interestingly, from their work we can infer the growth mechanism

[a]Author to whom correspondence should be addressed: Electronic mail: ncholu.manyala@up.ac.za (N. Manyala)

 

of multilayer graphite in which the second layer grows from below the first layer since the carbon source lies below the first layer, i.e. the bulk solid solution.

A quest to grow large-area graphene on metal substrates has led to the re-evaluation of these methods. Currently, CVD has emerged as a reliable fabrication method for large-area graphene on transition metals such as Ni and Cu.[9,15] The growth mechanisms of single-layer graphene on transition metals such as Ni, Ru, Ir and Cu are quite reasonable. Growth on Ni substrates involves the incorporation of carbon atoms into the bulk Ni substrate, followed by out-diffusion onto the Ni surface to form graphene layers when rapid cooling of the substrate occurs.[16–19] However, Ni has a fundamental limitation as the catalyst because it produces domains of single- and few-layered graphene with sizes of few to tens of micrometres. The graphene material is not homogeneous over the entire substrate due to the high solubility of carbon in Ni and because out-diffusion occurs mostly at the Ni grain boundaries. On transition metals such as Ru and Ir, single-layer growth occurs by supersaturation of a carbon adatom gas; the mechanism is independent of the carbon source and depends only on the adatom concentration.[19] Growth on Cu has been regarded as more viable for obtaining monolayer graphene, mainly by a surface-controlled process.[9,20] However, synthesizing uniform, defect-free multilayers has proved to be more difficult, and the growth mechanisms remain poorly understood.[19]

It has been observed that in the early stages of growth by CVD at atmospheric pressure, graphene forms as isolated "islands" which eventually coalesce to yield full, continuous monolayers. Occasionally these isolated islands are observed to have a second graphene layer which appears to nucleate at some sort of defect on the catalytic metal surface. It has often been assumed in the literature that the smaller islands are on top of the larger monolayer, and that they will grow and eventually form a second layer.[16,21–24] However, Tontegode and co-workers[25,26] had previously used Auger electron spectroscopy to suggest that graphene thick films grow in such a manner that the second and subsequent layers of graphene grow next to the substrate during segregation from Re-C solid solution and when carbon is deposited on Ir(111) in an inverted wedding cake fashion.[27] It has been shown that, once formed on the metal surface, graphene is not chemisorbed and detaches slightly from the surface, leaving room for intercalating particles.[28,29]

Recently, several groups have elucidated this underlayer growth mechanism of additional layers.[19,27,30,31] However, the methods used in these studies were expensive and complex. For example, Nie *et al.*[19] proved that second-layer islands nucleate between the existing layer and the substrate. This they did by monitoring misalignment during growth on Ir(111) using a low-energy electron diffraction (LEED) ultra-high vacuum chamber, angle-resolved photo-emission spectroscopy (ARPES) and low-energy electron microscopy (LEEM). The group later used the same techniques to prove underlayer growth of graphene islands on copper foil.[27] Li *et al.*[30] used carbon isotope-engineered samples with micro Raman spectroscopy and time-of-flight secondary ion mass spectrometry (TOF-SIMS) to prove the underlayer growth of the subsequent layers of graphene. The samples were exposed to $O_2$ plasma for 5 s in order to generate defects on the upper graphene layer to distinguish it from the layers beneath it, after which Raman spectroscopy was employed. TOF-SIMS was used for depth-profile analysis to image the sample isotope distribution and the stacking order on the as-grown multilayer graphene on Cu substrates.

The underlayer growth mechanism is readily understood from the perspective that during graphene growth, gas molecules may diffuse into the interface between the existing graphene and the metal substrate.[29,32,33] The weak interaction between graphene and its substrate, typically less than ~100 meV/C,[19] may provide the reason for the presence of molecules between the first layer of graphene and the metal substrate. Moreover, the CVD process of graphene growth relies on the substrate itself to generate the growth species by catalyzing hydrocarbon decomposition.[34]

In this paper we present a simple demonstration of under-growth of the second and subsequent graphene layers during CVD on Cu foil at atmospheric pressure. The novelty of this work is the use of a simple transfer mechanism of the CVD-grown graphene on a glass substrate and the exploitation of FE-SEM and AFM as diagnostic tools to prove this assertion. Furthermore, using a different approach, we clearly established the inverted wedding cake structure of the subsequent layers as suggested by Tontegode and co-workers[25,26] and later proved experimentally by Nie *et al.*[27]

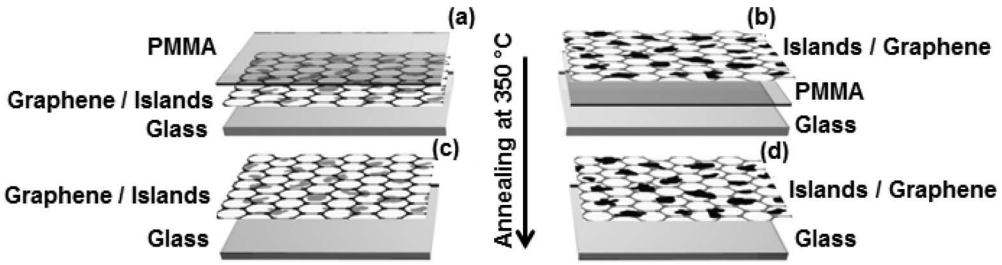


FIG. 1. Schematic diagram of graphene transfer: (a) direct-transfer (DT) to yield PMMA/graphene/glass; (b) inverse transfer (IT) to yield graphene/PMMA/glass; (c) and (d) removed PMMA after annealing of the samples in (a) and (b) respectively.

## II. EXPERIMENTAL

Graphene was grown by atmospheric pressure chemical vapor deposition (AP-CVD) in a quartz tube furnace from mixtures of $Ar:CH_4:H_2 = 300:15:9$ sccm gases at a temperature of 1000 °C on copper foil (25 $\mu$m thick foil, 99.8%, Alfa Aesar). The samples were rapidly cooled by pushing the quartz tube to the colder region of the furnace. They were then transferred to glass substrates using the bubbling method.[35] First, a thin layer of PMMA (average $M$w ~996 000 by GPC, Sigma-Aldrich Product No. 182265, dissolved in chlorobenzene with a concentration of 46 mg/mL) was spun-coated on the graphene/Cu samples at 4000 rpm for 10 s using a spin-coater, after which they were baked at 180 °C for 3 min to ensure good adhesion of the PMMA on the graphene/Cu.

The PMMA/graphene was separated from the copper foil using an aqueous solution of NaOH (0.1 M) as electrolyte in the electrolytic cell. A 10 V direct current (dc) voltage was applied across the cell containing the PMMA/graphene/Cu cathode and Fe wire anode. Hydrogen bubbles emerged at the PMMA/graphene/Cu interface and PMMA/graphene was separated from the copper foil. The PMMA/graphene was then scooped with polyethylene terephthalate (PET) into deionized water to remove any remaining NaOH particles.

The transfer to glass was done in two different ways. The first was direct transfer (DT): here the PMMA/graphene floating in water was scooped up from below with a glass substrate to yield a PMMA/graphene/glass configuration (see schematic Fig. 1(a)). The second was inverted transfer (IT): in this case, instead of scooping up the PMMA/graphene floating in water from below, the glass substrate was pressed against the PMMA/graphene from the top, ensuring that they stuck together, and then turned to yield a graphene/PMMA/glass configuration, where the graphene surface originally in contact with the Cu growth substrate was exposed (see schematic Fig. 1(b)). The samples were then annealed in an argon and hydrogen atmosphere ($Ar:H_2 = 300:9$ sccm) at 350 °C for 10 h to remove the PMMA. In this way we produced samples where both the top and bottom surfaces of the graphene could be inspected with a variety of microscopies (see schematic Fig. 1(c) and 1(d)).

A WITec alpha 300R+ confocal Raman system (WITec GmbH) was used for both imaging and spectroscopy with the laser power set below 2 mW in order to minimize heating effects. The excitation wavelength used was 532 nm (2.33 eV) through a numerical aperture of 0.9 and 100× magnification, which allows an image spatial resolution of about 360 nm. A high-resolution Zeiss Ultra Plus 55 FE-SEM operated at 1.0 kV was used to investigate the surface morphology of the graphene samples. The topographical images were obtained and the height analyses carried out using a Dimension Icon AFM (Bruker AXS) with NanoScope Analysis software in ScanAsyst mode. A total of five samples that were grown under the same conditions were examined in this study.

## III. RESULTS

Fig. 2(a) is an optical image of a DT graphene sample on a glass substrate; while Fig. 2(b) is the same image with the boundary of the graphene film indicated by a dotted line. The film was 2 cm × 2 cm in size, and it was electrically continuous over the full 2 cm length.

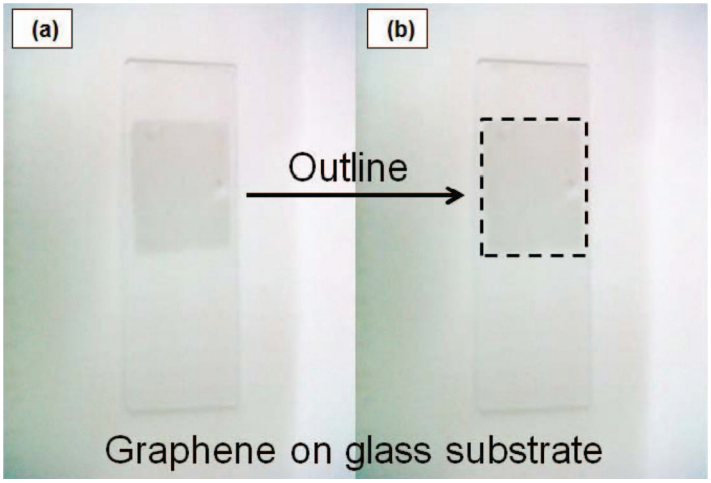


FIG. 2. (a) Optical micrograph of 2 cm × 2 cm graphene on glass, and (b) boundaries of the graphene sample in (a).

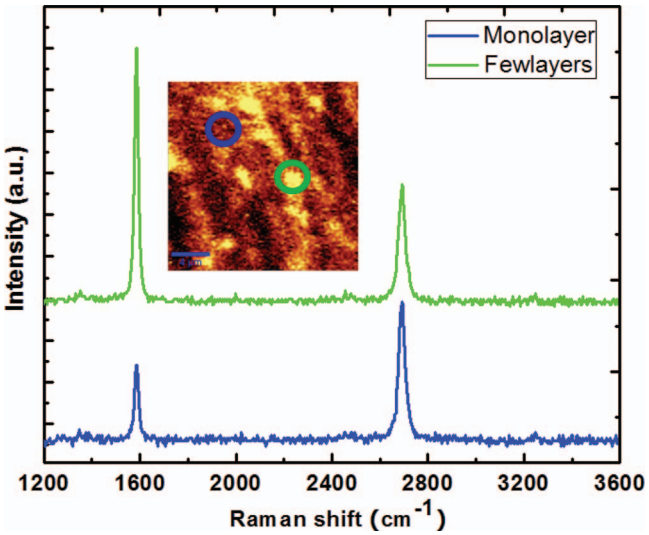


FIG. 3. Raman spectroscopy of the CVD graphene on glass substrate at two different spots indicated in the inset. (Inset) Raman map of the G-mode intensity showing a monolayer (blue circle) and few-layer graphene (green circle). Scale bar is 4 $\mu$m in the inset.

Raman spectroscopy is a useful diagnostic tool for determining the number of layers of graphene.[36,37] In particular, it has been established that the intensity ratio of the G and 2D peaks (1600 $cm^{-1}$ and 2700 $cm^{-1}$ respectively), together with the full width at half maximum (FWHM) of the 2D peak, may be used to infer the number of carbon layers. Monolayer regions are characterized by $I_{2D}/I_G$ ratio greater than one and FWHM of approximately $<50$ $cm^{-1}$, while a lower value of $I_{2D}/I_G$ and FWHM of approximately $>50$ $cm^{-1}$ indicate the presence of two or more layers.[36,37] Raman spectroscopy mapping was therefore used to establish that the films used for this work consisted of large monolayer regions interrupted by isolated regions of multilayer graphene. The inset to Fig. 3 shows a Raman map of the G -band intensity. Light (dark) regions correspond to higher (lower) G-band intensity, which is a signature of multilayer (monolayer) graphene. This interpretation is confirmed by the Raman spectra obtained at two different spots corresponding to the colored circles

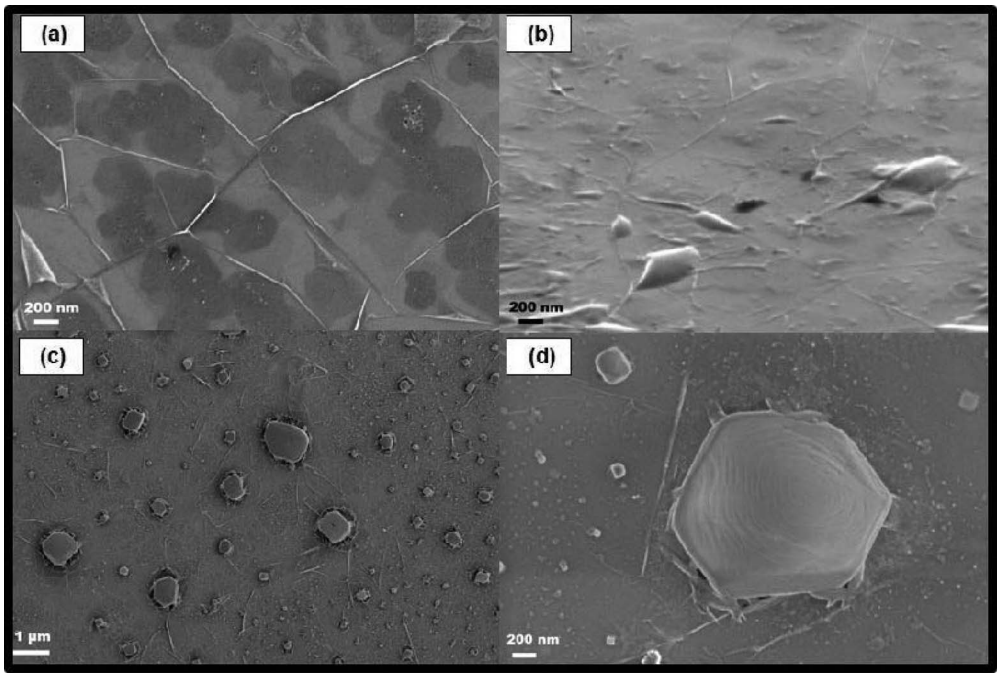


FIG. 4. FE-SEM images of: (a) direct-transfer (DT) graphene; (b) DT graphene on glass substrate taken at 70° with respect to the sample plane; (c) inverse-transfer (IT) graphene; and (d) high magnification of one of the islands in (c).

in the inset to the figure. The Raman spectra clearly show the expected dependence on graphene thickness: the calculated $I_{2D}/I_G$ and FWHM for few layer graphene represented by the green circle (upper spectrum) in Fig. 3 are 1.1 and 61 $cm^{-1}$ respectively, corresponding to two layers, and they are 1.8 and 40 $cm^{-1}$ respectively for the monolayer represented by the blue circle (lower spectrum) in Fig. 3. These results are consistent with what has been reported in the literature for both bilayer and monolayer graphene.[30]

Fig. 4(a) is FE-SEM image of the DT graphene revealing some patches that appear to be below a smooth, continuous graphene layer. The image suggests that these patches (which we refer to as graphene "islands") are underneath a continuous graphene monolayer, which is characterized by wrinkles that occur due to the different thermal expansion coefficients of graphene and copper foil.[38] The wrinkles seem to run continuously over some of the islands without a change in contrast. Ridges and swells are also visible in regions where adhesion between the film and the substrate is poor. As a simple proof that the ridges and swells are indeed on the top layer and the islands lie underneath them, FE-SEM image of DT graphene was taken while the sample was tilted at an angle of 70° with respect to the sample plane (see Fig. 4(b)). At this angle, the wrinkles and swells are more visible, while the islands or patches are no longer visible.

Fig. 4(c) is FE-SEM image of an IT graphene sample which clearly shows the multi-layer islands that lie on top of the monolayer graphene; the islands vary to some extent in size and shape but most are hexagonal (see Fig. 4(d)). The island in Fig. 4(d) exhibits a "concentric stacking" or "inverted wedding cake" structure. Our work proves this inverted wedding cake structure by showing that the DT and IT configurations image very differently in FE-SEM, contrary to the suggestion by Nie *et al.*[27] The concentric nature of the multilayer island suggests that all the layers in an island nucleate at a common site, perhaps associated with an impurity or special topography.[27] New layers nucleate next to the substrate, so the site remains active even when covered by the top monolayer graphene.[25,27]

AFM was used to further establish the underlayer growth process of subsequent layers and their inverted wedding cake structure. The inset to Fig. 5(a) shows an AFM image of DT graphene on a

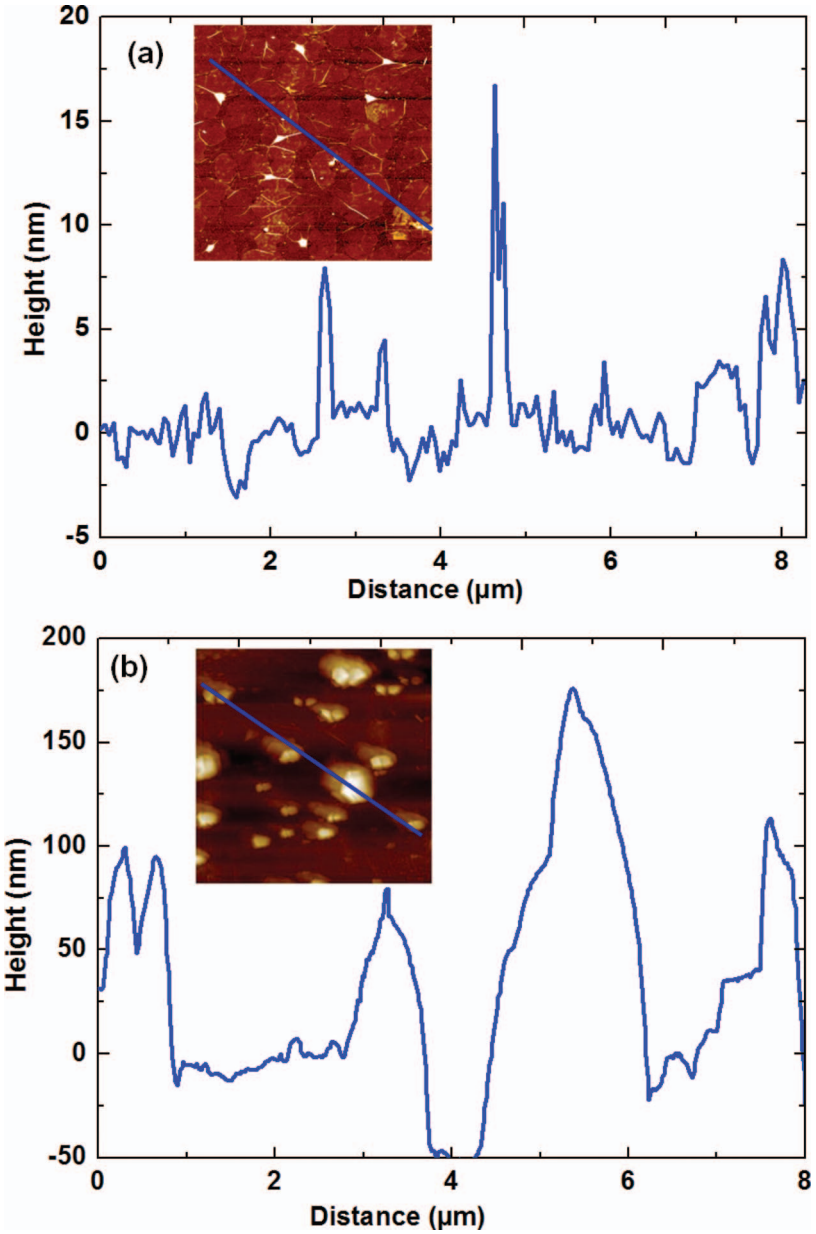


FIG. 5. (a) and (b): Cross-sectional plots of 7.2 $\mu$m $\times$7.2 $\mu$m 2D AFM images. (Insets) Height topographic for the DT and IT graphene samples respectively.

glass substrate, while the main figure is a line scan as indicated on the image. Here the patches of islands below the graphene, and the wrinkles, ridges and swells on top of graphene are visible. The line scan shows wider and relatively higher features which represent the islands that lie below the continuous monolayer. The heights of the features are relatively small (5–10 nm) and the scan shows considerable noise due to the presence of wrinkles on the top monolayer. Fig. 5(b) and its inset show a similar AFM image and line scan from a sample of IT graphene on glass, where the islands are expected to be on top of the continuous monolayer (see schematic in Fig. 1(b)). The line scan from this sample shows large and very high surface features compared with the DT sample. This is seen most vividly in Fig. 6, which shows a 3D AFM image of a large multilayer island exhibiting the inverted wedding cake phenomenon, similar to the SEM image shown in Fig. 4(d).

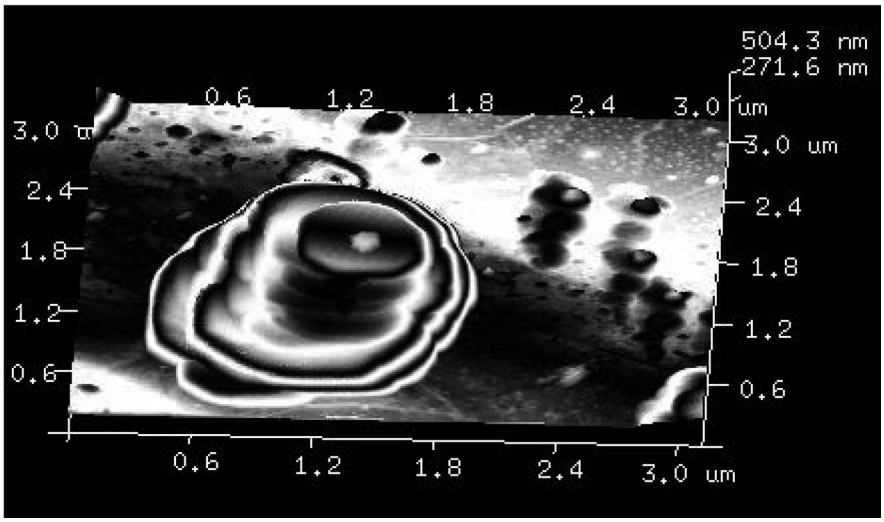


FIG. 6. 3D AFM image of one of the islands of the IT graphene sample.

## IV. CONCLUSION

We used a simple and direct approach based on scanning electron and atomic force microscopies to prove that indeed the subsequent graphene layers using the CVD method on Cu foil do grow underneath the first monolayer and that such layers form in an inverted wedding cake structure. This simple approach was made possible through two different methods of transferring graphene to glass substrates. The FE-SEM and AFM images of the inverse transfer (IT) samples clearly showed the hexagonal 3D islands with monolayer graphene below them - an inverted wedding cake-like structure. The concentric nature of the multilayer island suggests that all the layers in an island nucleate at a common site, perhaps associated with an impurity or special topography.[27] In some cases for IT samples, smaller graphene layers lie above the larger layers stacked like an inverted wedding cake, which becomes inverted in direct transfer (DT) samples.[25,27]

## ACKNOWLEDGMENTS

This study is based on research supported by the South African Research Chairs Initiative of the Department of Science and Technology (SARChI-DST) and the National Research Foundation (NRF). Any opinions, findings and conclusions, or recommendations expressed in this study are those of authors and therefore the NRF and DST do not accept any liability with regard thereto. MF thanks the Government of Lesotho, the University of Pretoria and the NRF for financial support for his study. A.T.C.J acknowledges support from the LRSM, through the U.S. National Science Foundation MRSEC, Grant No. DMR-1120901.

[1] K. S. Novoselov, A. K. Geim, S. V. Morozov, D. Jiang, Y. Zhang, S. V. Dubonos, I. V. Grigorieva, and A. A. Firsov, Science **306**, 666 (2004).
[2] A. K. Geim, Science **324**, 1530 (2009).
[3] P. Blake, D. P. Brimicombe, R. R. Nair, T. J. Booth, Da. Jiang, F. Schedin, L. A. Ponomarenko, S. V. Morozov, H. F. Gleeson, E. W. Hill, A. K. Geim, and K. S. Novoselov, Nano Lett. **8**, 1704 (2008).
[4] K. S. Kim, Y. Zhao, H. Jang, S. Y. Lee, J. M. Kim, K. S. Kim, J. H. Ahn, P. Kim, J. Y. Choi, and B. H. Hong, Nature **457**, 706 (2009).
[5] S. Y. Kwon, C. V. Ciobanu, V. Petrova, V. B. Shenoy, J. Bareno, V. Gambin, I. Petrov, and S. Kodambaka, Nano Lett. **9**, 3985 (2009).
[6] P. W. Sutter, J.-I. Flege, and E. A. Sutter, Nat. Mater. **7**, 406 (2008).
[7] J. Coraux, A. T. N'Diaye, C. Busse, and T. Michely, Nano Lett. **8**, 565 (2008).
[8] X. Li, W. Cai, J. An, S. Kim, J. Nah, D. Yang, R. Piner, A. Velamakanni, I. Jung, E. Tutuc, S. K. Banerjee, L. Colombo, and R. S. Ruoff, Science **324**, 1312 (2009).
[9] C. Mattevi, H. Kima, and M. Chhowalla, J. Mater.Chem. **21**, 3324 (2011).
[10] E. G. Acheson, United States Patent 568323 (1896).

[11] W. C. Arsem, Ind. Eng. Chem. **3**, 799 (1911).
[12] B. C. Banerjee, T. J. Hirt, and P. L. Walker, Nature **192**, 450 (1961).
[13] A. E. Karu and M. J. Beer, J. Appl. Phys. **37**, 2179 (1966).
[14] J. C. Shelton, H. R. Patil, and J. M. Blakely, Surf. Sci. **43**, 493 (1974).
[15] M. Losurdo, M. M. Giangregorio, P. Capezzuto, and G. Bruno, Phys. Chem. Chem. Phys. **13**, 20836 (2011).
[16] X. Li, W. Cai, L. Colombo, and R. S. Ruoff, Nano Lett. **9**, 4268 (2009).
[17] Q. Yu, J. Lian, S. Siriponglert, H. Li, Y. P. Chen, and S. S. Pei, Appl. Phys. Lett. **93**, 113103 (2008).
[18] A. Reina, X. Jia, J. Ho, D. Nezich, H. Son, V. Bulovic, M. S. Dresselhaus, and J. Kong, Nano Lett. **9**, 30 (2009).
[19] S. Nie, A. L. Walter, N. C. Bartelt, E. Starodub, A. Bostwick, E. Rotenberg, and K. F. McCarty, ACS Nano **5**, 2298 (2011).
[20] Z. Luo, Y. Lu, D. W. Singer, M. E. Berck, L. A. Somers, B. R. Goldsmith, A. T. Charlie Johnson, Chem. Mater. **23**, 1441 (2011).
[21] W. Wu, Q. Yu, P. Peng, Z. Liu, J. Bao, S. Pei, Nanotechnology **23**, 035603 (2012).
[22] C. Hwang, K. Yoo, S. J. Kim, E. K. Seo, H. Yu, and L. P. Bir, J. Phys. Chem. C **115**, 22369 (2011).
[23] I. Vlassiouk, M. Regmi, P. Fulvio, S. Dai, P. Datskos, G. Eres, and S. Smirnov, ACS Nano **5**, 6069 (2011).
[24] A. W. Robertson and J. H. Warner, Nano Lett. **11**, 1182 (2011).
[25] A. Y. Tontegode, Prog. Surf. Sci. **38**, 201 (1991).
[26] N. R. Gall, E. V. Rut'Kov, and A. Y. Tontegode, Int. J. Mod. Phys. B **11**, 1865 (1997).
[27] S. Nie, W. Wu, S. Xing, Q. Yu, J. Bao, S. Pei, K. F. McCarty, New J Phys. **14**, 093028 (2012).
[28] R. Rossei, M. De Crescenzi, F. Sette, C. Quaresima, A. Savoia, and P. Perfetti, Phys. Rev. B **28**, 1161 (1983).
[29] A. Y. Tontegode and E. V. Rut'kov, Phys. Usp. **36**, 1053 (1993).
[30] Q. Li, H. Chou, J. Zhong, J. Liu, A. Dolocan, J. Zhang, Y. Zhou, R. S. Ruoff, S. Chen, and W. Cai, Nano Lett. **13**, 486 (2013).
[31] W. Fang, A. L. Hsu, R. Caudillo, Y. Song, A. G. Birdwell, E. Zakar, M. Kalbac, M. Dubey, T. Palacios, M. S. Dresselhaus, P. T. Araujo, and J. Kong, Nano Lett. **13**, 1541 (2013).
[32] Y. Cui, Q. Fu, and X. Bao, Phys. Chem. Chem. Phys. **12**, 5053 (2010).
[33] R. Mu, Q. Fu, L. Jin, L. Yu, G. Fang, D. Tan, and X. Bao, Chem. Int. Ed. **51**, 4856 (2012).
[34] E. Loginova, N. C. Bartelt, P. J. Feibelman, and K. F. McCarty, New J Phys. **11**, 063046 (2009).
[35] L. Gao, W. Ren, H. Xu, L. Jin, Z. Wang, T. Ma, L. P. Ma, Z. Zhang, Q. Fu, L. Peng, X. Bao, and H. Cheng, Nature Commun. **3**, 699 (2012).
[36] A. C. Ferrari, Solid State Commun. **143**, 47 (2007).
[37] L. M. Malard, M. A. Pimenta, G. Dresselhaus, and M. S. Dresselhaus, Phys. Rep. **473**, 51 (2009).
[38] S. J. Chae, F. Gunes, K. K. Kim, E. S. Kim, G. H. Han, S. M. Kim, H. Shin, S. Yoon, J. Choi, M. H. Park, C. W. Yang, D. Pribat, and Y. H. Lee, Adv. Mater. **21**, 2328 (2009).